

Chapter 2

PZT Nano Active Fiber Composites-Based Acoustic Emission Sensor

Xi Chen and Yong Shi

Abstract A concept that utilizes the lead zirconate titanate (PZT) nano active fiber composites (NAFCs) to sense the acoustic emission (AE) for structural health monitoring (SHM) is demonstrated. The developed NAFCs consist of nanoscale PZT fibers with interdigitated electrodes on a silicon substrate. PZT nanofibers fabricated by an electrospinning process have a diameter of approximately 80 nm and aligned across the electrodes. Polydimethylsiloxane (PDMS) is severed as the polymer matrix and covers the sensor surfaces to protect nanofibers structures. The AE detection was demonstrated by both mounting the sensor on the surface of a steel table and embedding it in an epoxy structure. The output voltage reached the amplitude of 0.2 V in response to the acoustic wave generated by periodic impacts using a steel bar. The signal attenuation curves were measured to characterize the properties and demonstrate the anisotropic sensitivity of the PZT NAFCs sensor. The highly sensitive micro-sized PZT NAFCs sensors have promising applications in the SHM of composite structures such as the advanced carbon fiber-reinforced composites used in aerospace industry.

X. Chen · Y. Shi (✉)

Department of Mechanical Engineering, Stevens Institute of Technology,
Castle Point on Hudson, Hoboken, NJ 07030, USA
e-mail: Yong.Shi@stevens.edu

X. Chen

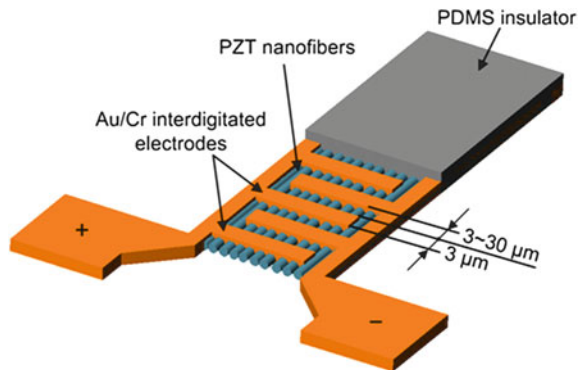
e-mail: xchen1@stevens.edu

2.1 Introduction

Recently, the application of carbon fiber composite structure has grown rapidly in the aerospace industry due to its high mechanical strength, high stiffness, and minimal weight [1, 2]. Being able to analyze and identify damages within composite structures using embedded sensors is highly desired [3]. Currently, strain gauges [4, 5], fiber optic sensors [6, 7], MEMS accelerometers [8], and piezoelectric acoustic emission (AE) sensors [9] are commonly used for structural health monitoring (SHM) applications. Piezoelectric sensors can achieve active sensing (excitation and sensing) [10] and the three other kinds of sensors are based on passive sensing. However, most of them are unsuitable for integrating into composites due to the small scale of the carbon fibers and the sensing technology. The active fiber composites (AFCs), developed first by Bent and Hagoood [11, 12], is one of the great candidates for this application. A similar lead zirconate titanate (PZT) fiber composite, macro fiber composites (MFCs) developed by NASA [13], has also been used for such purposes. The MFCs with micron-scale PZT fibers embedded in a polymer matrix have demonstrated a number of advantages compared to other AE sensors [9]. Compared with the carbon fibers involved, the larger diameter and high stiffness of PZT fiber make it difficult to embed into composite structures. A potential solution to this issue is to replace the micro size PZT fiber with nanoscale fiber in MFCs.

Piezoelectric AE sensors are designed using a direct piezoelectric effect. The sensitivity of these kinds of sensors is mainly determined by the piezoelectric voltage constant (g_{33}) of the piezoelectric materials. The polyvinylidene fluoride (PVDF) thin film-based AE sensors have much less sensitivity than PZT sensors and cannot be used at a high temperature [14]. PZT nanofibers prepared by an electrospinning process exhibit an extremely high piezoelectric constant, high bending flexibility, and high mechanical strength, which have been demonstrated in our previous work [15]. The g_{33} of PZT nanofiber is roughly 0.079 Vm/N [15] which is much higher than that of the PZT bulk (0.025 Vm/N) or PZT microfiber (0.059 Vm/N) [16]. For a given energy input of the elastic waves, PZT nanofiber can produce much higher voltage than the PZT microfiber, which results in a higher sensitivity of the sensor. Unlike the bulk or micro size PZT ceramic materials, the high flexibility allows PZT nanofiber to bend freely in a transverse direction. Thus, the PZT nanofiber-based AE sensor can be easily bonded to curved structures. When implemented in a practical application, the PZT nanofiber has a smaller chance of being damaged due to its small size, flexibility, and high mechanical strength, which can extend the lifetime of nanofiber-based devices. The latest developments of carbon nanotube (CNT) composite-based strain sensors [17, 18] provide a way to achieve the SHM of composite structures. However, the passive sensing technique requires a current passing through the sensor, which generates heat and costs more energy. The PZT nanofiber-based nanogenerator that can convert mechanical energy into electrical energy has been successfully

Fig. 2.1 Schematic view of the PZT NAFCs sensor. Reproduced from [1] by permission of the John Wiley and Sons (copyright 2011)



demonstrated in Ref [19] and illustrates the possibility of using the PZT nanofiber-based AE sensor to achieve the self-powered active sensing for SHM applications.

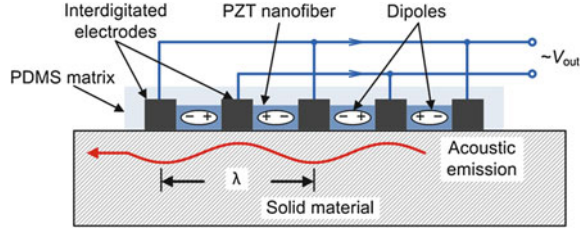
Here, we demonstrate an AE sensor that utilizes the PZT nano active fiber composites (NAFCs) for SHM. The developed PZT NAFC AE sensor consists of nanoscale PZT fibers with interdigitated electrodes on a silicon substrate. PZT nanofibers fabricated by an electrospinning process have a diameter varying from 60 to 85 nm and are aligned across the electrodes. Polydimethylsiloxane (PDMS) is served as the polymer matrix and cover the sensor surfaces to protect nanofibers structures. The AE detection was demonstrated by both mounting the sensor on the surface of a steel table and embedding it in an epoxy structure. The output voltage reached the amplitude of 0.2 V in response to the acoustic wave generated by the periodic impacts using a steel bar. The signal attenuation curves were measured to characterize the properties and demonstrate the anisotropic sensitivity of the PZT NAFCs AE sensor. The highly sensitive micro-sized PZT NAFCs AE sensors have promising applications in the SHM of composite structures such as the advanced carbon fiber-reinforced composites used in aerospace industry.

2.2 Design of PZT NAFCs AE Sensor

2.2.1 PZT NAFCs AE Sensor Concept

The concept of PZT NAFCs AE sensor is presented in Fig. 2.1. The PZT NAFCs sensor consists of nanofibers, interdigitated electrodes, and a polymer matrix. The PZT nanofibers are first aligned on a silicon substrate. The gold interdigitated electrodes are directly evaporated onto the surface of the PZT nanofibers, while the polymer layer is coated on top of the electrodes for mechanical integrity. The width of the deposited electrode was 3 μm and the gap between the two adjacent electrodes varied from 3 to 20 μm . The thickness of the whole sensor can be controlled within 2 μm when the PZT NAFCs AE sensor is released from the silicon substrate.

Fig. 2.2 The AE detection mechanism of PZT NAFCs. The figure shows the side view of the PZT NAFCs sensor mounted on a solid material to be monitored. The acoustic wave with a wavelength of λ illustrates the typical wave that PZT NAFCs can generate for the active sensing application. Reproduced from [1] by permission of the John Wiley and Sons (copyright 2011)



2.2.2 AE Detection Mechanism

The AE detecting mechanism of PZT NAFCs is illustrated in Fig. 2.2. The acoustic waves transferred through the structures, which induced elastic stress waves along the aligned nanofibers. The charge was separated in those nanofibers by the longitudinal stress waves, which resulted in a piezoelectric potential gradient along the nanofiber [20]. The generated piezoelectric potential $\sim V_{out}$ was picked up through the adjacent electrodes and transported to an external detection circuit.

The voltage generated between two adjacent electrodes of the PZT NAFCs can be calculated by

$$V_{out}^1 = \int g_{33}\varepsilon_{33}(l)E_p dl \quad (2.1)$$

where $\varepsilon_{33}(l)$ is the longitudinal strain along PZT nanofibers, l is the length of the nanofibers across the two adjacent electrodes, and E_p is the Young's modulus of PZT nanofibers. Assuming a perfect bonding between PZT nanofibers and PDMS polymer matrix, we have

$$\varepsilon_p = \varepsilon_m = \varepsilon_c \quad (2.2)$$

where ε_p is the strain in PZT nanofibers, ε_m and ε_c are the strains in the PDMS matrix and composite. Assuming both PZT nanofibers and PDMS matrix is elastic, the PZT NAFCs can be considered as unidirectional continuous fiber lamina. Therefore, we have

$$E_{33} = E_p v_p + E_m(1 - v_p) \quad (2.3)$$

$$v_p = A_p/A_c \quad (2.4)$$

where E_{33} is the longitudinal modulus, E_m is the Young's modulus of PDMS polymer, A_p is net cross-sectional area for the fibers, and A_c is the cross-sectional area for the PZT NAFCs. The major Poisson's ratio could be calculated as

$$\nu_{31} = \nu_{32} = \nu_p \nu_p + \nu_m(1 - \nu_p) \quad (2.5)$$

where ν_p and ν_m are the Poisson's ratio of PZT nanofibers and PDMS polymer, respectively. The longitudinal strain in the PZT nanofibers can be given as

$$\varepsilon_{33}(l) = \sigma_{33}(l)/E_{33} - \sigma_{11}(l)\nu_{31}/E_{33} - \sigma_{22}(l)\nu_{32}/E_{33} \quad (2.6)$$

where $\sigma_{11}(l)$, $\sigma_{22}(l)$ and $\sigma_{33}(l)$ are the stress functions in three directions. Thus, the output voltage can be rewritten as

$$V_{\text{out}}^1 = \int \left[\frac{\sigma_{33}(l)}{E_{33}} - \frac{\sigma_{11}(l)\nu_{31}}{E_{33}} - \frac{\sigma_{22}(l)\nu_{32}}{E_{33}} \right] E_p g_{33} dl \quad (2.7)$$

According to Eq. (2.7), the output voltage from the PZT NAFCs sensor is a function of the strength of the elastic wave. Since the PZT nanofibers were polled in opposite directions between each adjacent electrode (see Fig. 2.2), the output power was enhanced by the parallel connection of those units using an interdigitated pattern of electrodes. For the application of active sensing, the PZT NAFCs can generate elastic waves with the wavelength of λ , which is equal to twice the distance [21] between the electrodes as shown in Fig. 2.2.

2.3 Fabrication

2.3.1 PZT Nanofiber Synthesis

PZT nanofibers were prepared by electrospinning process [22, 23]. The starting material, PZT (52/48) sol-gel and poly vinyl pyrrolidone (PVP, Aldrich) were obtained from commercial sources. Alcohol was used as a solvent for PVP, while acetic acid was added to stabilize the solution and to control the hydrolysis reaction of the sol-gel precursor [24]. After being stirred vigorously for 2 h at room temperature, the mixture was fed into a microscale metallic tube through a syringe pump. A droplet of the modified sol-gel solution was held at the orifice of the metallic tube due to the high surface tension. A high DC voltage (10 kV) between the tip of the micro metallic tube and the collecting substrate was applied to overcome the surface tension and generate an electrically charged jet of the modified solution. After electrospinning, the as-spun nanofibers were annealed at 650 °C to obtain PZT nanofibers with the perovskite phase.

Figure 2.3 has shown the morphology and X-ray diffraction pattern of the annealed PZT nanofibers. Figure 2.3a was the scanning electron microscopy (SEM) image of a selected nanofiber with a diameter of 70 nm. By varying the

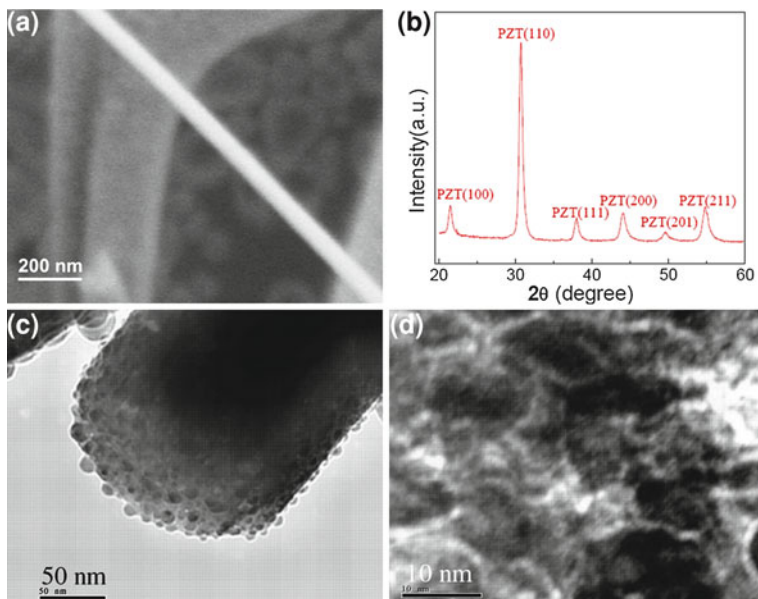


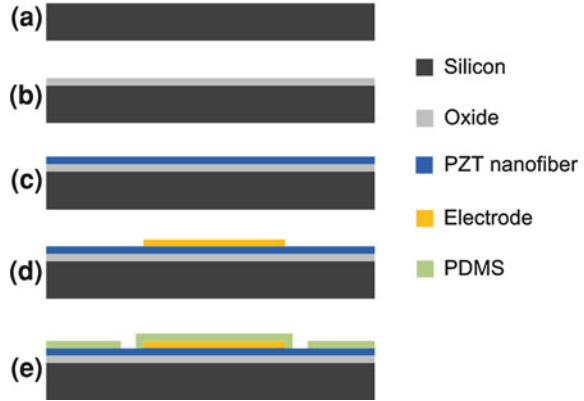
Fig. 2.3 **a** SEM image of single PZT nanofiber. **b** X-Ray diffraction pattern for the PZT nanofibers. **c** and **d** TEM images of a PZT nanofiber. Reproduced from [15] by permission of the American Institute of Physics (copyright 2009)

concentration of the polymer in the precursor, the average diameters of the nanofibers could be tuned from 52 ± 8 nm to 150 ± 12 nm. The X-ray diffraction (XRD) pattern of the annealed PZT nanofibers shown in Fig. 2.3b indicated that the PZT nanofibers annealed at 650 °C had pure perovskite phase. The annealing temperature was lower than that used by most other methods. Transmission electron microscopy (TEM) images of the cross-section and surface of PZT nanofibers were shown in Fig. 2.3c and d. The grain size of the PZT nanofibers was about 10 nm. The structure of the nanofiber seemed porous probably because of the polymer precursor solution of the sol–gel process [25]. By modifying the precursor and controlling the electrospinning parameters, a denser nanostructure could be obtained.

2.3.2 Fabrication of PZT NAFCs AE Sensor

The designed fabrication process is as shown in Fig. 2.4. A silicon wafer was used as the substrate to collect nanofibers and also to fabricate the composites (step a.). Then, a thin layer of thermal oxide was grown on the surface of the substrate as a diffusion barrier to prevent silicon transfer into the piezoelectric (PZT) fibers at elevated temperature and change their composition (step b.). Aligned piezoelectric

Fig. 2.4 Fabrication process of PZT NAFC AE sensor



nanofibers were deposited onto the substrate by electrospinning followed by an annealing process at 650 °C for 25 min (step c). A lift-off process was used to prepare interdigitated electrodes by using the photoresist of AZ5214 (step d). Polymer (PDMS) layer was deposited by spin coating (step e). Finally, the PZT nanofibers were polled by applying an electric field of 4 V/ μm across the interdigitated electrodes at a temperature of 140 °C for about 24 h.

As shown in Fig. 2.5, a millimeter size PZT NAFCs AE sensor was fabricated on a silicon substrate. After the annealing process, PZT nanofibers with a diameter of approximately 80 nm (see Fig. 2.5a) had a large concentration of perovskite phase as shown in the XRD pattern (inset in Fig. 2.5a). As shown in Fig. 2.5b, the PZT nanofibers were entirely covered by the thermally evaporated Au/Cr interdigitated electrodes to achieve a good connection. The width of the deposited electrode was 3 μm and the gap between the two adjacent electrodes varied from 3 to 20 μm .

By varying the size of interdigitated electrodes, the size of a single PZT NAFCs sensor cell can be fabricated from millimeter scale to microscale. Figure 2.6 shows a microscale sensor that has been fabricated.

After applying a thin PDMS layer as the matrix material on the top of the sensor, the wafer was cut to form the individual AE sensors. The finished PZT NAFCs sensor cells are as shown in Fig. 2.7. The silicon substrate was used as the rigid mechanical backing to avoid excessive stresses on PZT nanofibers and minimize the risk of damaging the electrical connection. The extraction copper wires were connected with the electrodes by using silver glue to connect with the external circuits. The PZT NAFCs AE sensor can be released from the silicon substrate by dry etching for different applications.

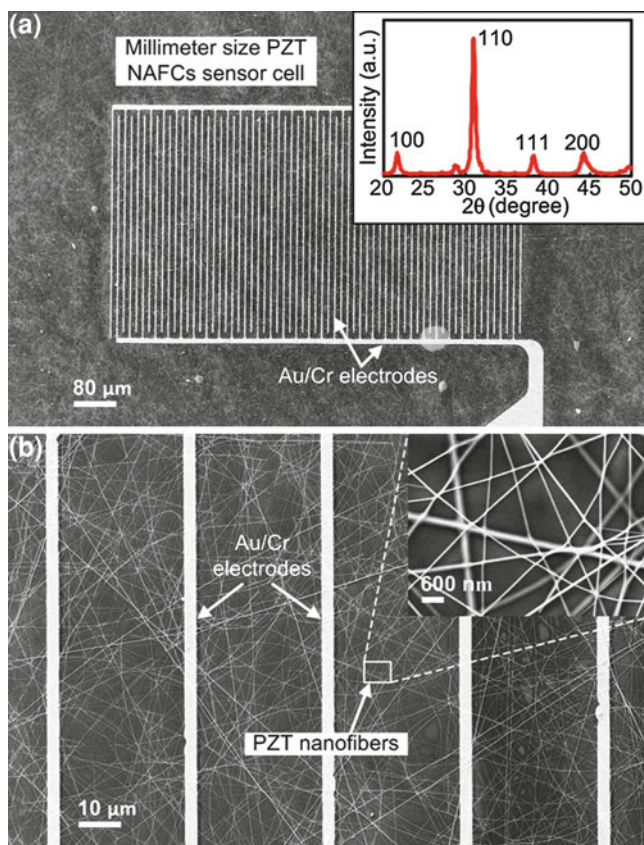


Fig. 2.5 **a** A SEM image of the millimeter size PZT NAFCs sensor cell before coating the PDMS layer. The inset in **a** shows the XRD pattern for the PZT nanofibers. **b** A SEM image of PZT nanofibers covered by Au/Cr interdigitated electrodes. The inset in **b** shows the diameter of PZT nanofiber is approximately 80 nm. Reproduced from [1] by permission of the John Wiley and Sons (copyright 2011)

Fig. 2.6 A SEM image of a micron size PZT NAFCs sensor cell. Reproduced from [1] by permission of the John Wiley and Sons (copyright 2011)

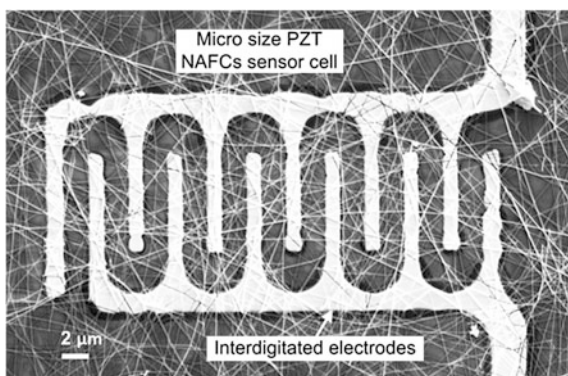
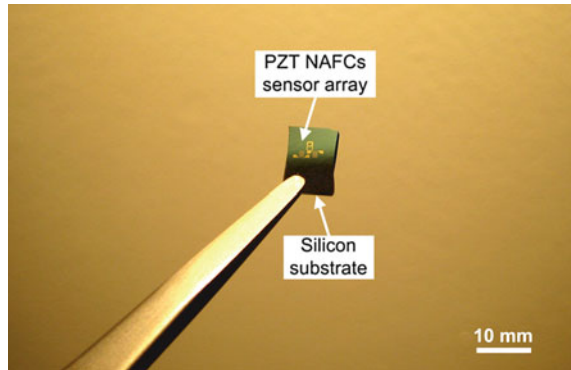


Fig. 2.7 An optical image of PZT NAFCs sensor cell array after coating a thin PDMS layer on the top surface. Reproduced from [1] by permission of the John Wiley and Sons (copyright 2011)



2.4 Characterization of PZT NAFCs AE Sensor

2.4.1 Elastic Wave Detection

A single AE sensor cell, with the width of $400\ \mu\text{m}$ and length of $800\ \mu\text{m}$, was selected to perform the measurement. The experiment was first carried out for the surface elastic wave detection. The PZT NAFCs was reversibly mounted on a grounded steel surface as shown in upper inset in Fig. 2.8. To eliminate the influence of the electromagnetic interference, the sensor structure was fully covered using a faraday cage. A grounded steel bar was used to generate the acoustic wave along the parallel direction of the nanofibers by periodic knocking on the steel surface. As shown in Fig. 2.8, the charge separation was recorded when the elastic wave reached to the NAFCs. The sensed signal was induced by piezopotential-driven transient flow of electrons under the stress of the substrate generated by the waves [26]. The higher the impact energy applied on the steel surface, the higher the voltage generated from the PZT NAFCs. The measured peaks were around $0.08\ \text{V}$ during the test and the signal vanished fast due to the low energy.

The PZT nanofiber composites were then embedded into a square-shaped epoxy structure and fine copper wires were utilized as the extraction electrodes to transport electrons to external circuit, see upper inset in Fig. 2.9. As shown in Fig. 2.9, the positive and negative voltage outputs were observed when a grounded steel bar was knocking on the epoxy structure and the voltages reached to $0.2\ \text{V}$ during the test. The negative voltage distribution was generated due to the reversely flowing carriers when the imbedded NAFCs suffering the restoring force from the structure oscillation after the external load was removed. Therefore, the PZT NAFCs AE sensor shows a promising application in SHM by integrating into structures.

Fig. 2.8 The voltage generation when used for surface elastic wave detection. Reproduced from [1] by permission of the John Wiley and Sons (copyright 2011)

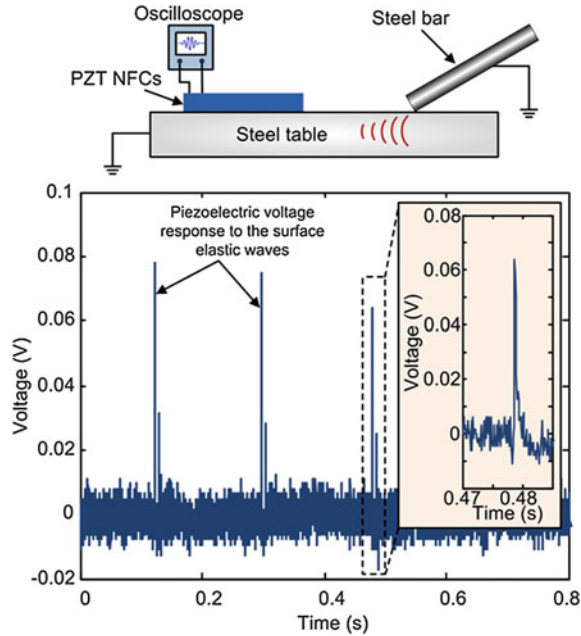


Fig. 2.9 The voltage generation when the PZT NAFCs was embedded in an epoxy structure. Reproduced from [1] by permission of the John Wiley and Sons (copyright 2011)

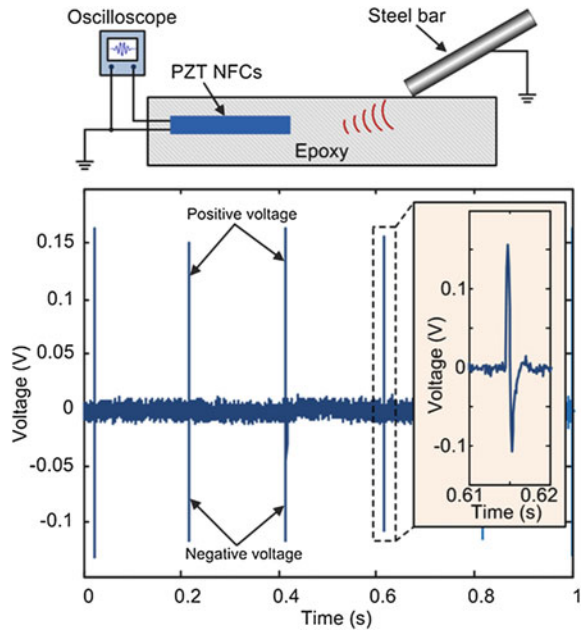
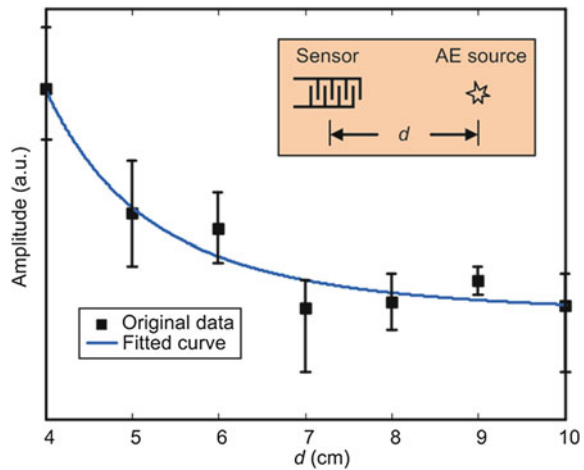


Fig. 2.10 Distance attenuation curve of the PZT NAFCs sensor as a function of distance between the AE source and the sensor. Reproduced from [1] by permission of the John Wiley and Sons (copyright 2011)

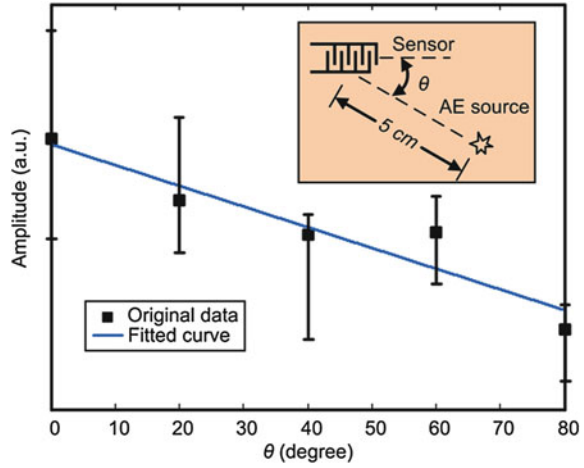


2.4.2 Signal Attenuation

In order to further study the sensing properties of the NAFCs sensor, the signal attenuation curves were measured by changing the location of the AE source on an isotropic Poly(methyl methacrylate) (PMMA) test plate. The signal attenuation test was first performed as a function of distance (d) along a direction parallel to the PZT NAFCs, as seen in the inset in Fig. 2.10. The PZT NAFCs were permanently bonded on the top surface of the PMMA test plate using epoxy. The AE signal was generated by utilizing the impact energy of a metal ball dropped on the test plate from a certain height. By varying the distance of AE source from 4 to 10 cm, the average amplitude of the output voltage was recorded at each location after several tests as shown in Fig. 2.10. From the measurement, it was determined that the values also depend on the shape of the PMMA plate and the sensor locations.

According to Eq. (2.7), the piezoelectric potential only indicates the longitudinal deformation of PZT nanofibers. The elastic waves along the nanofibers direction produce higher voltage than the waves normal to the fiber direction. The measurement of angular attenuation was then carried out by fixing the distance at 5 cm and changing the angles between the AE source and the sensor orientation. By varying the polar angle, the angular attenuation curve was measured as shown in Fig. 2.11. Therefore, the aligned nanofibers and interdigitated electrodes can lead to the anisotropic sensitivity of PZT NAFCs sensors. With the distance and angular attenuation properties, the AE source information can be easily identified using a small number of sensors.

Fig. 2.11 Angular attenuation curve of the PZT NAFCs as a function of angle between the AE source and the sensor. Reproduced from [1] by permission of the John Wiley and Sons (copyright 2011)

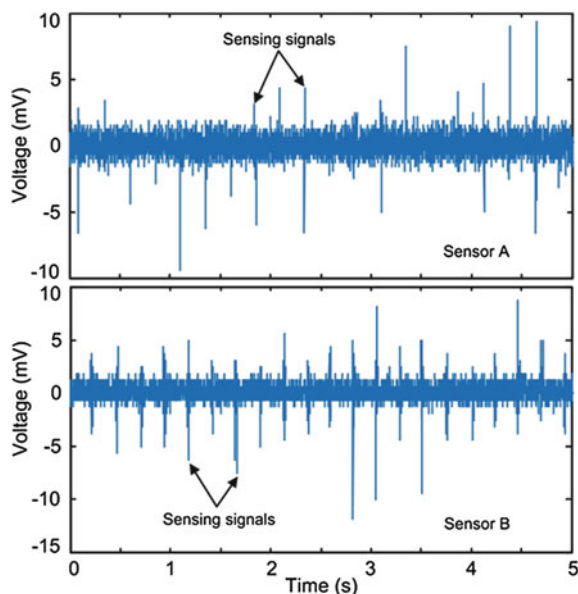


2.4.3 AE Detections of Micron Size Sensor

The AE detections of micron size PZT NAFCs sensors were also demonstrated by permanently mounting on the top surface of PMMA. For less PZT nanofibers and interdigitated electrodes, the sensitivity of micron size PZT NAFCs sensor is much lower than that of millimeter size sensor. SR560 preamplifier was used to amplify the generated voltage during the AE detection. A band-pass RC filter with cutoff frequencies of 300 Hz and 1 MHz was used to reduce the environmental noise to enhance the sensitivity of the sensor. Two micron size PZT NAFCs sensors, with the width of 15 μm and length of 30 μm , were used to sense the AE signal as shown in Fig. 2.12. With the source of periodic knocking on the PMMA surface using a steel bar, the amplitude of those sensors was about 10 mV which is much lower than that of the larger sensors described in the earlier section. The sensitivity can be enlarged by precisely designing the gaps between electrodes for different materials to be monitored [27].

During the test, all equipment and structures were well grounded in order to eliminate the influence of the bioelectric field of the human body and the electromagnetic interference from the testing equipment. The faraday cage was involved and well grounded during experiment. The amplitude of the noise signal was controlled under 2 mV. An interdigitated electrode based silicon substrate without PZT nanofibers had also been tested to verify the piezoelectric phenomena of NAFCs when subjected to the elastic waves. Although the surface charge of the devices could also create the potential difference, those signals can be eliminated by correct grounding.

Fig. 2.12 The demonstration of micron size PZT NAFCs used for acoustic emission detection. **a** The voltage generation when used for AE detection of sensor A. **b** The voltage generation when used for AE detection of sensor B. Reproduced from [1] by permission of the John Wiley and Sons (copyright 2011)



2.5 Conclusion

In conclusion, a new concept of using PZT NAFCs with interdigitated electrodes as AE sensors for SHM application was demonstrated. The diameter of PZT nanofibers was controlled at ~ 80 nm. The acoustic responses of the PZT NAFCs sensor were demonstrated by mounting the sensor on the surface of the steel table and embedding it in the epoxy structure. The peak voltage output reached 0.2 V in response to the acoustic wave generated by the periodic impacts using a grounded steel bar. The signal attenuation curves showed the anisotropic sensitivity of the PZT NAFCs sensor. The high sensitivity, microscale size, low weight, large flexibility, low cost, and anisotropic sensitivity make the PZT NAFCs sensors have a promising application in health monitoring by integrating them into composites. The active PZT materials also allow the possibility of the NAFCs sensor to achieve self-powered active sensing for the SHM application.

Acknowledgments This work was supported in part by the National Science Foundation (Award No. CMMI-0826418 & No. ECCS-0802168). The authors would also like to thank J. Li and G. Zhang for useful discussions.

References

1. Chen X, Li J, Zhang G et al (2011) PZT nanoactive fiber composites for acoustic emission detection. *Adv Mater* 23:3964
2. Lin M, Chang FK (2002) The manufacture of composite structures with a built-in network of piezoceramics. *Compos Sci Technol* 62:919

3. Giugliuti V, Redmond JM, Roach DP et al (2000) Active sensors for health monitoring of aging aerospace structures. *SPIE Proc* 3985:294
4. Perry CC (1987) Strain gauge measurements on plastics and composites. *Strain* 23:155–156
5. Tairova LP, Tsvetlov SV (1993) Specific features of strain measurement in composite materials. *Mech Compos Mater* 28:489–493
6. Singh H, Sirkis JS, Andrews J et al (1995) Evaluation of integrated optic modulator-based detection schemes for in-line fiber etalon sensors. *J Lightwave Technol* 13:1772
7. Todd MD, Johnson GA, Vohra ST (2001) Deployment of a fiber bragg grating-based measurement system in a structural health monitoring application. *Smart Mater Struct* 10:534
8. Adams DE (2007) Health monitoring of structural materials and components. Wiley, West Sussex
9. Barbezat M, Brunner AJ, Flueler P et al (2004) Acoustic emission sensor properties of active fibre composite elements compared with commercial acoustic emission sensors. *Sens Actuators A* 114:13
10. Park HW, Sohn H, Law KH et al (2007) Time reversal active sensing for health monitoring of a composite plate. *Sound Vib* 302:50
11. Bent A, Hagood NW (1995) Anisotropic actuation with piezoelectric fiber composites. *J Intell Mater Syst Struct* 3:338
12. Bent A, Hagood NW (1997) Piezoelectric fiber composites with interdigitated electrodes. *J Intell Mater Syst Struct* 8:903
13. Wilkie WK, Bryant RG, High JW et al (2000) Low-cost piezocomposite actuator for structural control applications. *Proc SPIE* 3991:323
14. Monkhouse RSC, Wilcox PW, Lowe MJS et al (2000) The rapid monitoring of structures using interdigital lamb wave transducers. *Smart Mater Struct* 9:304
15. Chen X, Xu SY, Yao N et al (2009) Potential measurement from a single lead zirconate titanate nanofiber using a nanomanipulator. *Appl Phys Lett* 94:253113
16. Swallow LM, Luo JK, Siores E et al (2008) A piezoelectric fibre composite based energy harvesting device for potential wearable applications. *Smart Mater Struct* 17:025017
17. Thostenson ET, Chou TW (2006) Carbon nanotube networks: sensing of distributed strain and damage for life prediction and self healing. *Adv Mater* 18:2837
18. Yamada T, Hayamizu Y, Yamamoto Y et al (2011) A stretchable carbon nanotube strain sensor for human-motion detection. *Nat Nanotechnol* 6:296
19. Chen X, Xu SY, Yao N et al (2010) 1.6 V nanogenerator for mechanical energy harvesting using PZT nanofibers. *Nano Lett* 10:2133
20. Xu S, Qing Y, Xu C et al (2010) Self-powered nanowire devices. *Nat Nanotechnol* 5:366
21. Monkhouse RSC, Wilcox PD, Cawley P (1997) Flexible interdigital PVDF transducers for the generation of Lamb waves in structures. *Ultrasonics* 35:489
22. Chen X, Yao N, Yong S (2011) Energy harvesting based on PZT nanofibers. In: Zhang L (ed) *Energy efficiency and renewable energy through nanotechnology*. Springer Series in Nanoscience and Technology
23. Xu SY, Shi Y, Kim SG (2006) Fabrication and mechanical property of nano piezoelectric fibers. *Nanotechnology* 17:4497–4501
24. Li D (2003) Xia Y (2003) Fabrication of tatania nanofibers by electrospinning. *Nano Lett* 3:555–560
25. Li D, Wang Y, Xia Y (2004) Electrospinning nanofibers as uniaxially aligned arrays and layer-by-layer stacked films. *Adv Mater* 16:361–366
26. Wang ZL (2010) Piezotronic and piezophototronic effects. *J Phys Chem Lett* 1:1388
27. Zhu W, Rose JL (1999) Lamb wave generation and reception with time-delay periodic linear arrays: a BEM simulation and experimental study. *IEEE Trans Ultrason* 46:654–664

Selected Topics in Micro/Nano-robotics for Biomedical
Applications

Guo, Y. (Ed.)

2013, XIV, 194 p., Hardcover

ISBN: 978-1-4419-8410-4